Proc. Natl. Acad. Sci. USA
Vol. 87, pp. 3338–3342, May 1990
Biochemistry

Polyoma virus small tumor antigen pre-mRNA splicing requires cooperation between two 3′ splice sites

HUI GE, JONATHAN NOBLE, JOHN COLGAN, AND JAMES L. MANLEY

Department of Biological Sciences, Columbia University, New York, NY 10027

Communicated by Joan A. Steitz, January 25, 1990 (received for review December 13, 1989)

ABSTRACT **We have studied splicing of the polyoma virus early region pre-mRNA *in vitro*. This RNA is alternatively spliced *in vivo* to produce mRNA encoding the large, middle-sized (MTAg), and small (StAg) tumor antigens. Our primary interest was to learn how the 48-nucleotide StAg intron is excised, because the length of this intron is significantly less than the apparent minimum established for mammalian introns. Although the products of all three splices are detected *in vitro*, characterization of the pathway and sequence requirements of StAg splicing suggests that splicing factors interact with the precursor RNA in an unexpected way to catalyze removal of this intron. Specifically, StAg splicing uses either of two lariat branch points, one of which is located only 4 nucleotides from the 3′ splice site. Furthermore, the StAg splice absolutely requires that the alternative MTAg 3′ splice site, located 14 nucleotides downstream of the StAg 3′ splice site, be intact. Insertion mutations that increase or decrease the quality of the MTAg pyrimidine stretch enhance or repress StAg as well as MTAg splicing, and a single-base change in the MTAg AG splice acceptor totally blocks both splices. These results demonstrate the ability of two 3′ splice sites to cooperate with each other to bring about removal of a single intron.**

Splicing of pre-mRNAs involves a two-step reaction that occurs in a complex multicomponent structure known as the spliceosome (for review, see refs. 1–3). In the first step of the reaction, the pre-mRNA is cleaved at the 5′ splice junction and the 5′ end of the intron is joined by a 2′-5′ phosphodiester linkage, or branch, to a nucleotide upstream of the 3′ splice site. This step thus consists of two half-reactions, which appear to occur in a concerted fashion, and generates two intermediates, the 5′ exon and the "lariat" intron–3′ exon. In the second step, the lariat intron–3′ exon is cleaved at the 3′ splice site and the 5′ and 3′ exons are then joined, in what also appears to be a concerted reaction.

The spliceosome (4–6) is a large RNA- and protein-containing structure that consists of four "small" nuclear ribonucleoprotein particles (snRNPs; the U1, U2, U4/U6, and U5) as well as additional proteins (for review, see ref. 7). Each snRNP contains one (U1, U2, and U5) or two (U4/U6) small RNA molecules, associated with on the order of 6–10 proteins, some of which are common to all snRNPs and others of which are specific to one or another snRNP. The U1 and U2 snRNPs interact with the pre-mRNA 5′ splice site and branch site, respectively. These interactions involve base pairing in mammals (8–10) as well as in yeast (11–13). The U4/U6 and U5 snRNPs join the complex later, perhaps as a preformed subcomplex (14, 15). Although a protein component of U5 snRNP may contact the 3′ splice site (16, 17), the U4/U6 snRNP, in which the two RNAs are initially tightly associated with each other by base pairing, appears not to contact the pre-mRNA directly (18). A number of additional proteins also likely play a role in the splicing reaction (e.g., refs. 19–22).

The complexity and size of the splicing apparatus suggests that steric constraints may play a role in splicing of some pre-mRNAs. Consistent with this proposal, several studies have shown that introns in higher eukaryotes have a minimum size requirement. Roughly 45 nucleotides (nt) must separate the 5′ splice site and branch point (23–27), and the minimum distance between the branch point and 3′ splice site appears to be approximately 18 nt (26, 28). The simian virus 40 small tumor antigen pre-mRNA contains an intron of 66 nt in which both the 5′ splice site–branch point and branch point–3′ splice site are at or near these minimums (26, 29). These limiting distances play an important role in modulating the relative amounts of small and large tumor antigen mRNAs produced from the alternatively spliced simian virus 40 early pre-mRNA.

The early region of the related DNA tumor virus, polyoma, encodes three proteins, the small, middle-sized, and large tumor antigens (StAg, MTAg, and LTAg, respectively) (30). These are produced by alternative splicing of a common precursor containing a single intron, utilizing different pairs of 5′ and 3′ splice sites (see Fig. 1). The MTAg and StAg introns, which share a common 5′ splice site but use different 3′ splice sites, are both unusually small. The MTAg intron size (62 nt) approximates the limit defined above, but the StAg intron (48 nt) is significantly below the minimum. To investigate the mechanism by which this exceptionally small intron is excised, we have studied polyoma early pre-mRNA splicing *in vitro*. Surprisingly, StAg splicing requires that the 3′ splice site used for MTAg splicing, which lies downstream of the StAg intron, be functional. These results have interesting implications concerning the mechanism of splicing as well as the selection of alternative splice sites.

MATERIALS AND METHODS

Plasmid Constructions. The DNA template for the wild-type (PY2) precursor RNA (pre-RNA) was constructed by inserting a *Bst*XI–*Eco*RI (nt 167–1562) fragment of the polyoma early region into the polylinker of pGEM-3. For the 5′ truncated template lacking the LTAg 5′ splice site (ΔT), an *Sph* I–*Eco*RI fragment (nt 698–1562) was inserted into pGEM-3. The MTAg polypyrimidine stretch deletion mutants ΔT^{Δ} and $PY2^{\Delta}$ were made by deleting a *Ban* II–*Mae* I fragment (nt 796–807) from the ΔT and Py2 plasmids. The insertion mutants ΔT^{py} and $PY2^{py}$ were created by inserting a synthetic 15-mer, which corresponds to the polypyrimidine stretch from the adenovirus 2 late leader sequence, into the ΔT and Py2 *Mae* I sites at nt 807. An *Mae* I–*Alu* I fragment from adenovirus 2 (nt 7036–7101) was cloned into the ΔT *Mae* I site at nt 807 to create the plasmid ΔT^{i66}. A single-base substitution mutant that changes the MTAg AG to AA (808A)

The publication costs of this article were defrayed in part by page charge payment. This article must therefore be hereby marked "*advertisement*" in accordance with 18 U.S.C. §1734 solely to indicate this fact.

Abbreviations: StAg, polyoma small tumor antigen; MTAg, polyoma middle-sized tumor antigen; LTAg, polyoma large tumor antigen; snRNP, small nuclear ribonucleoprotein particle; nt, nucleotide(s).

was kindly provided by T. Benjamin (Harvard Medical School) and subcloned as above. Nucleotide sequences of all mutants were verified by the dideoxynucleotide method.

Preparation of Transcripts and *in Vitro* Splicing. Full-length plasmids (Py2 series) were cleaved with *Pvu* II and truncated plasmids (ΔT series) were cleaved with *Xmn* I. Precursor RNAs were transcribed with SP6 RNA polymerase in the presence of 7-methylguanosine(5')triphospho(5')guanosine (m^7GpppG) and [α-^{32}P]GTP. For the production of high specific activity uniformly labeled pre-RNAs for fingerprinting, transcription reactions contained 250 μCi (1 Ci = 37 GBq) of each ribonucleotide triphosphate (31). Nuclear extracts were prepared by a modification of the method of Dignam *et al.* (32) in which the dialysis buffer contained 42 mM $(NH_4)_2SO_4$ instead of 0.1 M KCl (31). Both HeLa and 293 cells were used to produce extracts (31). The products obtained with the two types of extracts were qualitatively identical, although slightly more of the StAg and MTAg RNAs were obtained with 293 extracts. Splicing reactions and analysis of products by gel electrophoresis were performed as described (31).

Branch Point Mapping. Lariat and debranched LTAg, MTAg, and StAg introns were eluted from denaturing preparative polyacrylamide gels and digested with RNase T1 exactly as described (31). The resulting oligonucleotides were resolved by electrophoresis through a 25% polyacrylamide/8 M urea gel. T1 RNA fingerprinting and secondary analyses using RNase A were also performed as described (31).

RESULTS

Two related DNA templates were constructed to produce polyoma early region pre-mRNAs for *in vitro* processing (Fig. 1). The Py2 plasmid encodes a precursor RNA of ≈1 kilobase, which includes all the information required for LTAg, MTAg, and StAg splicing. Py ΔT pre-RNA is only 210 nt long and cannot make the LTAg splice because the 5′ splice site is deleted. The rationale for using this pre-RNA stemmed in part from previous experiments demonstrating that *in vitro* splicing of simian virus 40 small tumor antigen RNA is activated by deletions that remove the LTAg 5′ splice site (31, 33). Fig. 1 also displays the relevant sequences of several mutants used in these experiments. Although they are shown in the ΔT background, most of them have also been analyzed in Py2 constructs.

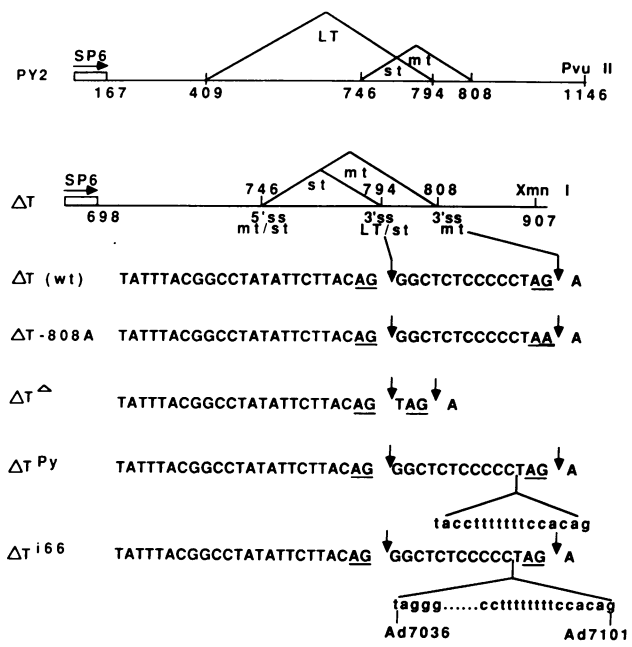

FIG. 1. Schematic diagram of polyoma early region and relevant nucleotide sequences of wild-type (wt) and mutant templates. The structures of the Py2 and ΔT precursors are indicated at the top of the figure. The SP6 RNA polymerase promoter and restriction sites used to produce run-off transcripts are shown. The numbers are from the polyoma virus nucleotide sequence (30). The LTAg (LT), MTAg (mt), and StAg (t) introns and the positions of the 5′ and 3′ splice sites (ss) are indicated. The arrows denote the positions of the StAg/LTAg and MTAg 3′ splice sites, and the AG dinucleotides are underlined. Ad7036 and Ad7101 are nucleotide numbers from the adenovirus DNA sequence (30).

Characterization of Polyoma *in Vitro* Splicing Products. To determine whether all of the possible products of polyoma virus early splicing can be formed *in vitro*, Py2 and ΔT precursors were synthesized and incubated in HeLa or 293 cell nuclear extract (31, 32) and analyzed by polyacrylamide gel electrophoresis (Fig. 2*A*). To aid in identification of products, purified RNAs were analyzed both with and without enzymatic debranching (34) prior to electrophoresis. Somewhat unexpectedly, products of all three splices were produced from the Py2 pre-RNA. LTAg intermediates and products were all well-resolved, and the MTAg and StAg introns were clearly detected. Note that two species of similar mobilities, both designated as a StAg intron, were observed in the absence of debranching (see also Fig. 3). Experiments described below suggest that they reflect the utilization of distinct branch sites during StAg splicing. The MTAg and StAg splicing efficiencies were increased slightly when the Py ΔT pre-RNA was used, and the splicing products and intermediates were better resolved from the pre-RNA. However, the StAg and MTAg spliced RNAs and the lariat 3′ exon intermediates remained poorly resolved from one another and gave rise to somewhat diffuse bands (see also Fig. 3). This is at least in part due to the fact that these RNAs are all very similar in size.

To verify the identities of several of the RNAs indicated in Fig. 2*A*, high-specific-activity Py2 and ΔT pre-RNAs were synthesized, processed, and debranched as above, and all introns and 5′ exons were purified from preparative polyacrylamide gels. (The two StAg species were not resolved in these gels.) These RNAs were digested with RNase T1 and subjected to two-dimensional fingerprint analysis (data not shown) or, for the introns, one-dimensional analysis on 25% polyacrylamide/urea gels (Fig. 2*B*). These results, coupled with secondary analysis with RNase A of many of the T1 oligonucleotides (data not shown), revealed that the structures indicated are correct and also the location of the branch points used in LTAg, MTAg, and StAg splicing. Specifically, LTAg splicing uses a single branch point, an adenosine in an 8-mer T1 oligo (indicated 8* in Fig. 2*B*), located 19 nt upstream of the LTAg 3′ splice site. Splicing to MTAg also uses a single branch point, an adenosine in a 15-mer T1 oligo (15* in Fig. 2*B*), which is located 18 nt upstream of the MTAg 3′ splice site. This site, however, is only 4 nt upstream of the LTAg/StAg 3′ splice site. Two branch points are used in StAg splicing. The predominant one is the same as used by LTAg—i.e., the adenosine 19 nt from the 3′ splice site. Unexpectedly, a branch was also detected in the T1 15-mer (indicated by the * in Fig. 2*B*). The mobilities of this oligonucleotide and the corresponding debranched form (indicated OH_{15}) were reduced due to the absence of a phosphate at the end of the intron. Secondary analysis of both branched and debranched forms of this oligonucleotide confirmed that it lacked a 3′ phosphate and also revealed that branching occurred at the same adenosine utilized in MTAg splicing (data not shown). In the StAg intron, this residue is situated only 4 nt from the 3′ splice site. Fig. 2*C* displays the structure of the T1 oligonucleotides and also indicates the sequences of the two branch sites. Each shares a five out of six match with the metazoan branch site consensus sequence (35–37).

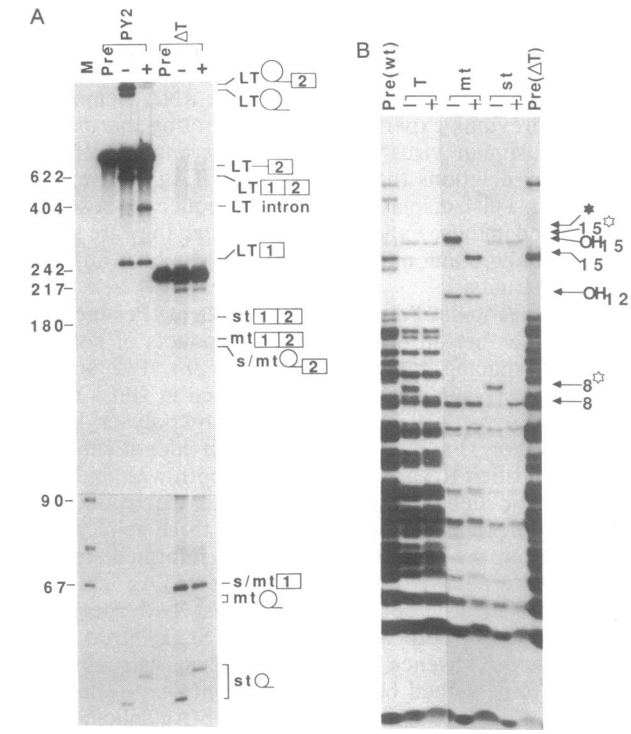

C LT 5'SS

G / UAAG / AAG / G / CUACAUG / ..... / CACAG / CG / UG /

st/mt5'SS

UAUAAUCCAAG / UAAG / UAUCAAG / AG / G / G / CG / G / G /

8 LT/st 15 mt/(st) LT/st3'SS 12 mt3'SS

UAUUUACG / G / CCUAUAUUCUUACAG / G / G / CUCUCCCCCUAG

branch site		distance from 3' AG
LT / st*	UAUUUAC	19
mt / (st)	UUCUUAC	18, (4)
consensus	YNYURAY	18–37

FIG. 2. Characterization of polyoma early pre-mRNA splicing products. (*A*) *In vitro* splicing of Py and ΔT pre-RNAs. Py2 and ΔT ^{32}P-labeled precursors were synthesized and processed *in vitro*, and the products were fractionated on a denaturing 6% polyacrylamide gel either without (−) or with (+) prior debranching. Lanes: Pre, precursor RNA; M, ^{32}P-labeled *Hpa* II digest of pBR322. Molecular sizes (in nt) are indicated on the left. The structures of substrates, intermediates, and products are shown on the right. (The lower part of the gel was exposed to x-ray film four times longer than the top to facilitate detection of intron products.) LT, LTAg; mt, MTAg; st, StAg. (*B*) RNase T1 analysis of excised introns. Both undebranched (−) and debranched (+) introns were recovered from preparative gels and digested to completion with RNase T1. The resulting oligonucleotides were separated in a 25% polyacrylamide/8 M urea gel. Lanes: Pre(wt), RNase T1 digest of Py2 precursor; Pre(ΔT), RNase T1 digest of ΔT precursor. The sizes (in nt) are indicated on the left. OH indicates T1 oligonucleotides from the 3' ends of the introns, which have reduced mobilities due to the lack of a 3' phosphate. Oligonucleotides containing a branched nucleotide are indicated by open and solid stars. The RNA marked by the solid star is the branched 15-mer from the 3' end of the StAg intron. (*C*) Partial nucleotide sequence of the Py2 precursor from the LTAg 5' splice site (LT 5'SS) to the MTAg 3' splice site (mt 3'SS), including the entire sequence of the StAg and MTAg introns, is shown. The expected RNase T1 cleavage fragments are bracketed by slashes, and the sequences with homology to the mammalian branch site consensus are underlined. The branch points used during *in vitro* splicing are indicated by asterisks. At the bottom, the match of the branch sites to the consensus sequence and distances between 3' splice sites and the two branch points are indicated. The + indicates the predominant StAg branch site. Y, pyrimidine, R, purine, N, any nucleotide.

Mutations in the MTAg 3' Splice Site Influence StAg as Well as MTAg Splicing. The utilization in StAg splicing of a branch point only 4 nt upstream of the 3' splice site and its coincidence with the branch point used in MTAg splicing suggested the possibility that StAg splicing in some way makes use of sequences at the MTAg 3' splice site. To test this, several mutations in the MTAg 3' splice site were constructed and analyzed (see Fig. 1), initially in the ΔT background to facilitate analysis of their effects on StAg and MTAg splicing. ΔT^{Δ} deletes 11 of the nucleotides that separate the two 3' splice sites, and ΔT^{Py} contains a 17-nt insertion immediately upstream of the MTAg 3' splice site. The inserted nucleotides are derived from the adenovirus late L1–L2 3' splice site (30), which contains an excellent polypyrimidine stretch. It was expected that the ΔT^{Δ} mutations would eliminate MTAg splicing, whereas ΔT^{Py} would enhance this splice due the increased size of the intron and the improved quality of the 3' splice site. The interesting question was how these mutations would affect StAg splicing. They could be predicted to have no effect, if selection of one or another of the two 3' splice sites is unlinked; opposite effects, if selection of 3' splice sites is competitive; or the same effect, if there is cooperation between the two splice sites—a possibility raised by the distinct StAg branch point described above. The appropriate pre-RNAs were processed *in vitro* and analyzed by gel electrophoresis with or without debranching. The results, shown in Fig. 3*A*, provide strong support for the latter possibility. StAg, as well as MTAg, splicing was greatly

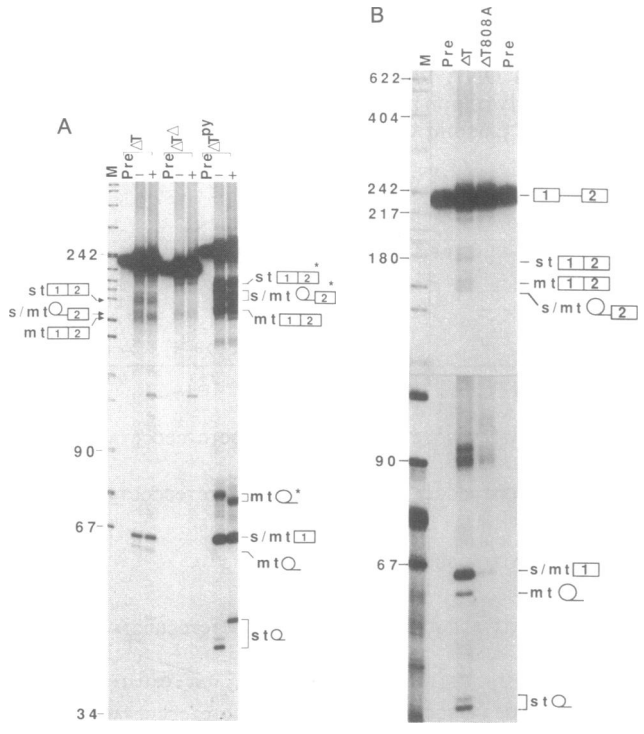

FIG. 3. Mutations in the MTAg (mt) 3' splice site affect StAg (st) splicing. (*A*) Effects of mutations in the MTAg polypyrimidine stretch. ΔT, ΔT^{Δ}, and ΔT^{Py} precursors were processed and analyzed by electrophoresis on a denaturing 7% gel with (+) and without (−) prior debranching. Lanes: Pre, unprocessed precursor; M, DNA size markers. The products are indicated schematically on the right. Asterisks indicate expanded products resulting from the insertion in ΔT^{Py}. (*B*) Effects of a single-base change in the MTAg AG splice acceptor. The indicated precursors were processed and analyzed (without debranching) as in *A*. The bottom half of the gel was exposed four times longer than the top to facilitate comparison of intron products. The origin of the bands at approximately 90 nt is not known. However, they were not detected reproducibly (e.g., see Fig. 4) and may represent degradation products.

reduced by the deletion mutation in ΔT^{Δ}. Even more strikingly, StAg and MTAg splices were both significantly enhanced by the 17-nt insertion in ΔT^{Py}: all products and intermediates of both splices were readily detectable.

The above results indicate that a strong MTAg 3′ splice site facilitates StAg splicing. To determine whether this reflects a requirement for an intact AG at the MTAg 3′ splice site as well as a strong polypyrimidine stretch, we analyzed the splicing potential of the mutant ΔT-808A, which contains a single-base substitution changing this AG dinucleotide to AA (see Fig. 1). This mutation was originally constructed and analyzed by Liang *et al.* (38), who showed that not only was the accumulation of MTAg protein in infected cells blocked but also, and more unexpectedly, the ratio of LTAg to StAg was increased. The products of ΔT wild-type and ΔT-808A *in vitro* splicing are compared in Fig. 3*B*. The results show that both MTAg and StAg splicing were inhibited by the mutation, indicating that the downstream MTAg AG is indeed required for StAg splicing.

LTAg Splicing Is not Affected by Mutations of the MTAg 3′ Splice Site. LTAg and StAg splicing utilize the same 3′ splice site. Therefore, even though there are no size constraints on LTAg splicing, and LTAg does not utilize the MTAg branch site, it was nonetheless possible that LTAg splicing might be influenced by the MTAg 3′ splice site mutations that affect StAg splicing. To test this possibility, the mutations analyzed above were introduced into the Py2 plasmid, and pre-RNAs were synthesized and processed *in vitro*. Analysis of the products, shown in Fig. 4, revealed that LTAg splicing was not significantly affected by any of the mutations tested (results with Py2-808A not shown). Note that the mutation in $Py2^{Py}$ enhanced StAg and MTAg splicing to such an extent that intermediates and products of these splices were produced efficiently even in competition with LTAg splicing. We conclude that the requirement for the downstream MTAg 3′ splice site is unique to StAg splicing.

A Strong Distal 3′ Splice Site can Block StAg Splicing. The mutation in ΔT^{Py} increases both the quality of the MTAg 3′ splice site and the distance separating the StAg and MTAg 3′ splice sites from 14 to 28 nt. Since StAg splicing not only occurred but was actually enhanced by this mutation, it is clear that the distance between the two 3′ splice sites can be increased by at least 14 nt without deleterious effects on StAg splicing. To determine whether insertion of a strong 3′ splice site even farther downstream could also enhance StAg splicing, the mutant ΔT^{i66} was constructed (see Fig. 1). This insertion mutant also contains the strong adenovirus L1–L2 3′ splice site, but in addition intron sequences extending upstream for a total of 66 nt. The net effect of this mutation was to introduce this strong 3′ splice site 77 nt downstream of the StAg 3′ splice site, leaving intact the MTAg 3′ splice site. The products of *in vitro* processing of this pre-RNA, with and without debranching, are shown in Fig. 5. The results indicate that ΔT^{i66} pre-RNA was spliced very efficiently, using the StAg/MTAg 5′ splice site and the inserted 3′ splice site, resulting in removal of the 125-nt expanded "MTAg" intron. Strikingly, not only was StAg splicing not enhanced by this efficient splice, but use of both StAg and MTAg 3′ splice sites was completely inhibited. Thus, a strong, downstream 3′ splice site appears to block StAg splicing, presumably by a *cis*-competition mechanism.

DISCUSSION

The results described above indicate that splicing of polyoma virus early pre-RNA to produce StAg mRNA takes place by an unusual mechanism. Specifically, StAg splicing requires that the downstream MTAg 3′ splice site be functional, and StAg splicing is in fact enhanced by a mutation that increases the quality of the MTAg 3′ splice site. These findings not only offer an explanation for how this anomalously small intron can be excised but also suggest that the association of splicing factors with the pre-mRNA might be more flexible than was previously thought.

Both the MTAg and StAg introns are unusually short. The MTAg branch point is located 18 nt upstream of the 3′ splice site and 44 nt from the 5′ splice site. These distances are in keeping with the minimums described in other systems and indicate that the MTAg intron is a conventional, albeit short, intron. The StAg intron, however, is quite different. The results presented above indicate that StAg splicing can proceed by two pathways, defined by the location of the branch point. The most prominent utilizes a branch point 19 nt upstream of the 3′ splice site, which results in a subthreshold 5′ splice site to branch point distance of 29 nt. In the minor pathway, the 5′ splice site to branch point distance is the same 44 nt as in MTAg, but the branch point to 3′ splice site

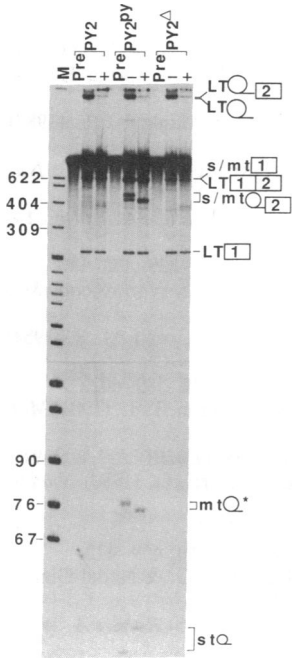

FIG. 4. MTAg (mt) 3′ splice site does not influence LTAg (LT) splicing. The indicated Py2 pre-RNAs were spliced *in vitro* and the products were analyzed on a denaturing 6% polyacrylamide gel. Lanes: Pre, precursor; M, DNA size markers. Products are indicated schematically on the right, with the asterisk denoting the expanded MTAg (mt) intron produced from $Py2^{Py}$. (The lower half of the gel was exposed four times longer than the top.)

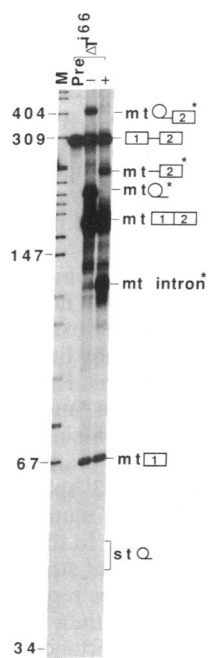

FIG. 5. A strong distal 3′ splice site inhibits StAg (st) splicing. ΔT^{i66} pre-RNA was spliced *in vitro* and the products were analyzed by electrophoresis on a denaturing 7% gel. The sizes of the DNA marker fragments are indicated on the left in nt. The structures of the precursor, intermediates, and the products are schematically shown on the right. The expanded intron products are indicated by asterisks. The predicted position of the StAg intron is indicated by brackets. mt, MTAg.

distance is only 4 nt, dramatically shorter than the previously observed minimum of 18 nt.

How mechanistically might the MTAg intron 3′ splice site facilitate StAg splicing? Perhaps the most straightforward model can be envisaged for the pathway utilizing the MTAg branch point. We suggest here that factors associate with the pre-mRNA in the initial stages of spliceosome assembly utilizing MTAg signals. This may involve binding of the protein factor U2AF (22) to the MTAg polypyrimidine stretch, which facilitates binding of U2 snRNP to the MTAg branch site. The remaining steps of spliceosome assembly and the first step of the splicing reaction proceed normally. The second step is atypical, in that either one of two AG dinucleotides can be selected for 3′ splice site cleavage and ligation to the 5′ exon. Although several studies (39–41) have shown that multiple AGs can be used in conjunction with a single branch site, in these instances, the upstream AGs were preceded by purines rather than the consensus pyrimidine (42), and the AGs were very close together. In the polyoma pre-mRNA, both AGs follow a pyrimidine, and they are separated by 14 nt. The use of both of these AGs may reflect a "scanning" mechanism that normally uses the first AG downstream of the branch site (43), but in this case the StAg AG is used inefficiently because of the extremely short 4-nt distance separating it and the branch point. In any event, the fact that a functional 3′ splice site can be located only 4 nt downstream from the lariat branch point has important implications regarding the mechanism of pre-mRNA splicing in higher eukaryotes, in that it suggests there is not a significant steric constraint on the distance separating nucleotides involved in the first step in splicing (the branch site) and the second (the 3′ splice site).

It is more difficult to envision how the major StAg splicing pathway, which utilizes the upstream branch point that is shared with LTAg splicing, is facilitated by a downstream 3′ splice site. How can the MTAg 3′ splice site compensate for the prohibitively short 29-nt distance separating the branch point and 5′ splice site? One possibility is that the back-to-back 3′ splice sites function cooperatively. For example, perhaps U2AF, or the U5-associated intron-binding protein (16, 17), binds to these two sites cooperatively, and the resulting tighter interaction better stabilizes U2 snRNP binding to the lariat branch site, which would otherwise be sterically hindered by U1 snRNP bound to the 5′ splice site. Although the ability of splicing factors to function cooperatively has not been tested to date, we note that the 17-nt insertion that increased StAg (and MTAg) splicing efficiency created a 21/22-nt polypyrimidine stretch at the MTAg 3′ splice site, which is consistent with the proposal that factor interactions involving the polypyrimidine stretch are important for facilitating StAg splicing. However, whatever the mechanism for the splice site cooperation, it is important to note that it apparently cannot function over a considerable distance, as insertion of a strong 3′ splice site 77 nt downstream was competitive, not cooperative.

Is cooperation between splice sites a phenomenon of general significance? While it is clear that this will not be the standard mechanism, we are aware of one other example of this phenomenon, which suggests that it is not limited to facilitating the splicing of unusually small introns. Krainer *et al.* (44) analyzed the *in vitro* splicing of a mutant β-thalassemic globin pre-mRNA that contained a single-base change creating an AG 18 nt downstream of the branch point in the first intron, 20 nt upstream of the natural 3′ splice site. Although splicing occurred exclusively to the mutant AG, deletion of the natural AG prevented splicing. In this case, perhaps the mutant 3′ splice site is of insufficient strength to function alone. The natural 3′ splice site may be required to activate lariat formation, but the mutant AG is then selected by a "scanning" mechanism. It will be of importance in the future to determine not only how frequently splice site cooperation occurs but also the mechanisms involved.

We are grateful to C. Prives for suggesting that analysis of polyoma early region splicing might be informative. We also thank T. Benjamin for pointing out the properties of the polyoma virus mutant 808A and providing us with the DNA. This work was supported by Grant CA33620 from the National Institutes of Health.

1. Padgett, R. A., Grabowski, P. J., Konarska, M. M., Seiler, S. & Sharp, P. A. (1986) *Annu. Rev. Biochem.* **55**, 1119–1150.
2. Green, M. R. (1986) *Annu. Rev. Genet.* **20**, 671–708.
3. Krainer, A. & Maniatis, T. (1988) in *Frontiers in Transcription and Splicing*, eds. Hanes, B. D. & Glover, D. M. (IRL, Oxford), pp. 131–206.
4. Brody, E. & Abelson, J. (1985) *Science* **228**, 963–967.
5. Grabowski, P. J., Seiler, S. & Sharp, P. A. (1985) *Cell* **42**, 345–353.
6. Frendewey, D. & Keller, W. (1985) *Cell* **42**, 355–367.
7. Steitz, J. A., Black, D. L., Gerke, V., Parker, K. A., Kramer, A., Frendeway, D. & Keller, W. (1988) in *Structure and Function of Major and Minor Small Nuclear Ribonucleoprotein Particles*, ed. Brinstiel, M. L. (Springer, Berlin), pp. 115–154.
8. Zhuang, Y. & Weiner, A. M. (1986) *Cell* **46**, 827–835.
9. Zhuang, Y. & Weiner, A. M. (1989) *Genes Dev.* **10**, 1545–1561.
10. Wu, J. & Manley, J. L. (1989) *Genes Dev.* **10**, 1553–1561.
11. Parker, R., Siliciano, P. G. & Guthrie, C. (1987) *Cell* **49**, 229–239.
12. Seraphin, B., Kretzner, L. & Rosbash, M. (1988) *EMBO J.* **7**, 2533–2538.
13. Siliciano, P. G. & Guthrie, C. (1988) *Genes Dev.* **2**, 1258–1267.
14. Cheng, S.-C. & Abelson, J. (1987) *Genes Dev.* **1**, 1014–1027.
15. Konarska, M. M. & Sharp, P. (1987) *Cell* **49**, 763–774.
16. Tazi, J., Alibert, C., Temsamani, J., Reveillaud, I., Cathala, G., Brunel, C. & Jeanteur, P. (1986) *Cell* **47**, 755–766.
17. Gerke, V. & Steitz, J. A. (1986) *Cell* **47**, 973–984.
18. Bindereif, A. & Green, M. R. (1987) *EMBO J.* **6**, 2415–2424.
19. Krainer, A. R. & Maniatis, T. (1985) *Cell* **42**, 725–736.
20. Kramer, A. (1988) *Genes Dev.* **2**, 1155–1167.
21. Swanson, M. S. & Dreyfuss, G. (1988) *EMBO J.* **7**, 3519–3529.
22. Ruskin, B., Zamore, P. D. & Green, M. R. (1988) *Cell* **52**, 207–219.
23. Wieringa, B., Hofer, E. & Weissman, C. (1984) *Cell* **37**, 915–925.
24. Ulfendahl, P. J., Petterson, U. & Akusjarvi, G. (1985) *Nucleic Acids Res.* **13**, 6299–6315.
25. Ruskin, B., Greene, J. M. & Green, M. R. (1985) *Cell* **41**, 833–844.
26. Fu, X.-Y., Colgan, J. & Manley, J. L. (1988) *Mol. Cell. Biol.* **8**, 3582–3590.
27. Smith, C. W. & Nadal-Ginard, B. (1989) *Cell* **56**, 749–758.
28. Reed, R. & Maniatis, T. (1985) *Cell* **41**, 95–105.
29. Fu, X.-Y. & Manley, J. L. (1987) *Mol. Cell. Biol.* **7**, 738–748.
30. Tooze, J. (1981) *DNA Tumor Viruses* (Cold Spring Harbor Lab., Cold Spring Harbor, NY), 2nd Ed.
31. Noble, J. C. S., Pan, Z.-Q., Prives, C. & Manley, J. L. (1987) *Cell* **50**, 227–236.
32. Dignam, J. D., Lebovitz, R. M. & Roeder, R. G. (1983) *Nucleic Acids Res.* **11**, 1475–89.
33. van Santen, V. L. & Spritz, R. A. (1986) *Nucleic Acids Res.* **14**, 9911–9926.
34. Ruskin, B. & Green, M. R. (1985) *Science* **229**, 135–140.
35. Keller, E. B. & Noon, W. A. (1984) *Proc. Natl. Acad. Sci. USA* **81**, 7417–7420.
36. Ruskin, B., Krainer, A. R., Maniatis, T. & Green, M. R. (1984) *Cell* **38**, 317–331.
37. Zeitlin, S. & Efstratiadis, A. (1984) *Cell* **39**, 589–602.
38. Liang, T. F., Carmichael, G. G. & Benjamin, T. L. (1984) *Mol. Cell. Biol.* **4**, 2774–2783.
39. Fu, X.-Y., Ge, H. & Manley, J. L. (1988) *EMBO J.* **7**, 809–917.
40. Ulfendahl, P. J., Kreivi, J. P. & Akusjarri, G. (1989) *Nucleic Acids Res.* **17**, 925–938.
41. Reed, R. (1989) *Genes Dev.* **3**, 2113–2123.
42. Mount, S. M. (1982) *Nucleic Acids Res.* **10**, 459–472.
43. Smith, C. W. J., Porro, E. B., Patton, J. G. & Nadal-Ginard, B. (1989) *Nature (London)* **342**, 243–247.
44. Krainer, A., Reed, R. & Maniatis, T. (1985) *Robert A. Welch Conf. Chem. Res.* **29**, 353–382.